Prediction of moisture content and energy consumption in microwave drying of beef based on an optimized SSA-BP model

Jing Ling[1], Jie Xu[2*], Dennis R. Heldman[3], Ting Wu[1]

(1. *School of Computer Science, Guangzhou Maritime University, Guangzhou 510725, China*;
2. *Department of Biological Systems Engineering, Washington State University, Pullman, WA 99164, USA*;
3. *Department of Food Science and Technology, The Ohio State University, Columbus, OH 43210, USA*)

Abstract: This study investigates the application of an enhanced Back-Propagation (BP) neural network model for analyzing and predicting beef microwave drying processes. Based on Fick's second law of diffusion, effective moisture diffusivity was determined under varying microwave power levels (70-420 W) and relative humidity conditions (0%, 30%, 50%). Experimental results revealed moisture diffusivity values ranging from 2.23×10^{-9} to 2.87×10^{-8} m^2/s. A significant inverse relationship was observed between microwave power and specific energy consumption, with optimal energy efficiency (8.39 MJ/kg water) achieved at 420 W. A multi-layer BP neural network architecture was developed to model drying kinetics and energy consumption patterns, with subsequent optimization using Sparrow Search Algorithm (SSA) for weight and threshold parameter calibration. Comparative analysis demonstrated that the SSA-optimized BP neural network significantly outperformed both conventional BP models and genetic algorithm-optimized variants in predictive accuracy. The enhanced model exhibited robust performance in predicting moisture content evolution and energy consumption dynamics throughout the drying process. These findings provide valuable insights for developing energy-efficient industrial-scale beef drying systems while maintaining product quality. The proposed intelligent computing framework represents a promising approach for precise modeling, prediction, and optimization of microwave drying processes in food processing applications.

Keywords: microwave power, SSA-BP, specific energy consumption, moisture content, prediction
DOI: 10.25165/j.ijabe.20251804.9832

Citation: Ling J, Xu J, Heldman D R, Wu T. Prediction of moisture content and energy consumption in microwave drying of beef based on an optimized SSA-BP model. Int J Agric & Biol Eng, 2025; 18(4): 312–320.

1 Introduction

Beef jerky is a popular snack made from sliced whole-muscle meat that undergoes curing and drying processes. This method not only enhances flavor but also reduces moisture content, which helps inhibit microbial growth. By lowering water activity, jerky can be stored for extended periods without refrigeration, making it a convenient and portable protein source[1-3]. For microbiological safety and shelf-stability, beef jerky products require a moisture content between 10-50 g per 100 g of product, with water activity below 0.85[4].

For drying purposes, the modern meat processing industry employs multiple techniques such as hot air, microwave, and vacuum drying[5]. While conventional hot air drying remains predominant, it presents significant limitations including color deterioration, compromised rehydration capacity, nutritional degradation, flavor alterations, and accelerated lipid oxidation[6-8]. These quality issues necessitate exploring alternative drying technologies.

The ongoing advancements in drying technologies have positioned microwave drying as a significant and actively researched area within agricultural and food processing[9]. This technique offers notable advantages over conventional hot air drying, effectively mitigating some of its inherent limitations and substantially enhancing the drying efficiency of agricultural commodities[10]. During microwave drying, the polar molecules within the material selectively absorb microwave radiation energy, leading to rapid volumetric heating. This internal energy conversion generates pressure gradients that promote efficient moisture migration from the product's interior to its surface, resulting in accelerated and effective drying[11,12].

To optimize meat drying processes for enhanced energy efficiency, productivity, and product quality, a comprehensive understanding of moisture transport phenomena is essential[3,13]. However, experimental investigations are resource-intensive and time-consuming. Meat dehydration complexity is influenced by multiple factors including drying parameters, processing conditions, sample characteristics, and pretreatment methods[14]. While semi-empirical and empirical models have been used to describe drying kinetics[5], their applicability is often limited to specific conditions, with meat dehydration complexity frequently exceeding their predictive capacity[15].

Artificial Neural Networks (ANNs), particularly Back-Propagation (BP) networks, have demonstrated superior capabilities in modeling complex food processing operations[15,16].

Their ability to model non-linear relationships without requiring explicit prior knowledge of the system has led to

Received date: 2025-04-07 **Accepted date:** 2025-05-13
Biographies: Jing Ling, Associate Professor, research interest: intelligent detection and intelligent information processing, Email: lingjing0519@163.com; **Dennis R. Heldman**, Professor, research interest: application of engineering principles and concepts to the manufacturing of foods with minimum energy, water and waste, Email: heldman.20@osu.edu; **Ting Wu**, MS candidate, research interests: intelligent detection and intelligent information processing, Email: 45636214@qq.com.

***Corresponding author: Jie Xu**, Postdoc Researcher, research interest: food science, microbiology, and engineering. Department of Biological Systems Engineering, Washington State University, Pullman, WA 99164, USA, Email: jie.xu42@email.wsu.edu.

successful applications in various drying scenarios. Examples include the characterization of microwave-dried thyme leaves[17], the prediction of energy and exergy parameters during mushroom slice drying, and the modeling of physicochemical changes in dried root vegetables[18], with high correlation coefficients (R>0.80). The microwave drying process of meat presents unique analytical challenges due to its inherent characteristics as a small sample dataset exhibiting complex nonlinear relationships between moisture content and energy consumption parameters.

Back-Propagation (BP) networks, while effective for modeling complex non-linear relationships, are susceptible to limitations such as slow convergence and entrapment in local minima, largely dependent on the optimization of weights and thresholds. Various optimization algorithms, including Genetic Algorithms (GAs)[19], Particle Swarm Optimization (PSO)[20], and Sparrow Search Algorithm (SSA)[21], have been employed to address these challenges. The SSA method offers enhanced advantages for BP network optimization. SSA's superior global search capability, faster convergence rates, and a more robust balance between exploration and exploitation enable more efficient and accurate training, leading to improved model generalization compared to other methods.

In addition, improving drying processes by reducing energy consumption and providing high quality with minimal increase in economic input has become the goal of modern drying[22]. Therefore, the aim of this study was to study the effects of microwave power on drying kinetics, specific energy consumption, and modeling of drying of beef. The present study addresses these challenges by integrating advanced machine learning techniques with BP neural networks to develop an improved predictive model for microwave drying of beef. The research objectives encompass:

1) Systematic investigation of drying characteristics under varying microwave power levels (70-420 W) and relative humidity conditions (0%-50%);

2) Development and validation of an enhanced BP neural network architecture for precise prediction of moisture content evolution and energy consumption patterns;

3) Comparative analysis with existing neural network models to establish optimal modeling frameworks for microwave drying processes.

2 Materials and methods

The experimental data were collected during microwave drying of lean beef tenderloin samples. A Galanz-G90F23 microwave oven (Guangdong Galanz Electrical Appliances Manufacturing Co., Ltd., China) was used for sample treatment. A LQ-W50002 electronic analytical balance (UKO-weight Electronic Technologies Ltd., UK) was used to measure the sample mass in relation to drying time. The system consisted of three subsystems: an online mass-monitoring microwave heating system, a unidirectional airflow control system for moisture evacuation, and a humidity measurement system, as shown in Figure 1. The equipment has a microwave magnetron frequency of 2450 MHz, and provides a maximum output of 900 W. The microwave oven was equipped with an electronic balance and provided real-time transmission and storage of sample mass as moisture was removed during drying.

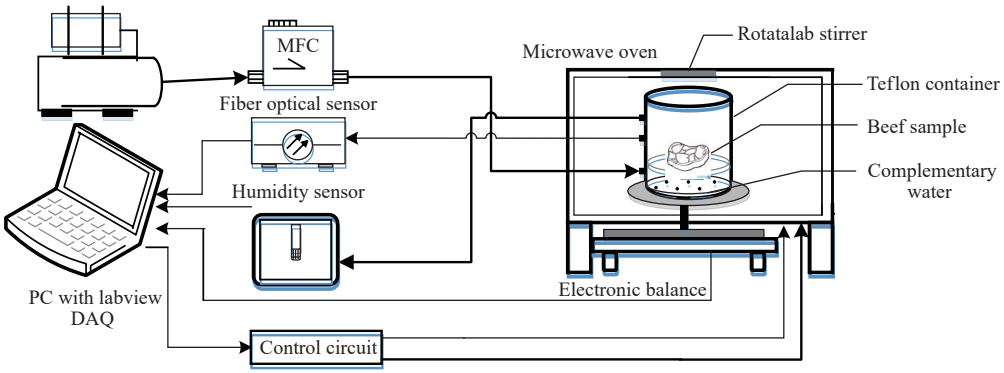

Figure 1 Structural diagram of experimental drying system

2.1 Experimental methods and data acquisition

The initial sample mass and moisture content (using AOAC procedures) were determined[23]. The initial moisture content was (73.4±0.5)% (wet basis), initial mass was 25±0.05 g, and the sample thickness was 10±0.5 mm. The final moisture content of sample in this study was set to 25% (wet basis) based on the requirements of general commercial dried beef jerky (USDA resource)[24]. Experimental data were collected at six microwave power levels (70 W, 140 W, 210 W, 280 W, 350 W, and 420 W) and three relative humidity levels (0%, 30%, and 50%) at room temperature. Single-factor test analysis method was employed and grouped microwave drying data according to different relative humidity levels and power levels [25].

To address the issue of controlling the convection air humidity during the microwave drying process, a modified Galanz-G90F23 microwave oven (Guangdong Galanz Electrical Appliances Manufacturing Co., Ltd.) was used to develop a new microwave drying system. The modified microwave oven had a 900 W magnetron, with the cathode and anode plates powered by independent power supplies, allowing for linear adjustment of the microwave power output from 0 to 900 W. A rotating stirrer installed inside the microwave cavity ensured more uniform microwave irradiation. Beef samples were housed in a sealed cylindrical Teflon container, measuring 100 mm in diameter and 130 mm in height. The sidewall of the container is equipped with ports for air intake, exhaust, and fiber optic sensor installation. Comparable experimental methods have been used to explore the impact of relative humidity on the microwave drying process of agricultural products[25-27].

The container was mounted on an electronic analytical balance (LQ-W50002, UKO-weight Electronic Technologies Ltd., UK) supported by a pedestal and a Type-I support frame, enabling ongoing tracking of the sample mass during the drying process. Compressed air, maintained at a temperature between 23°C and 25°C and dried using a desiccant, was supplied to the sample container via a Teflon pipeline from a compressor (OutStanding,

750-30L, China). Airflow rate, crucial for maintaining stable relative humidity, was regulated by a mass flow controller (SevenStar, MFC D07-19C, China) installed between the compressor and the container. To prevent condensation prior to humidity measurement, a thermal insulation pipeline and chamber were installed downstream of the sample container. As the compressed air expelled moisture from the container, a high-precision electronic hygrometer (Vaisala, HMT130) was selected for the experiment to ensure accurate measurement of the relative humidity within the sample container. For control and recording purposes, data on power, mass, and relative humidity were updated and transmitted to a host computer every 10 seconds.

2.2 Modeling of drying process

The drying rate (V_{DR}) of the sample was estimated as follows[12]:

$$V_{DR} = \frac{M_{t+\Delta t} - M_t}{\Delta t} \quad (1)$$

where, V_{DR} stands for the drying rate; $M_{t+\Delta t}$ is the moisture content (g water/g dry matter) at $t+\Delta t$; Δt is an incremental time (s) for a defined variation in moisture content.

Specific energy consumption can be calculated using the following equation[28]:

$$E_{mic} = \frac{t_{on} P \times 10^{-6}}{m_v} \quad (2)$$

where, E_{mic} is the specific energy consumption in MJ/kg [H_2O].

2.3 Effective moisture diffusivity

Moisture diffusion within the product involved diffusion of liquid or vapor. A widely accepted mechanism used to describe the characteristics is Fick's second law[29]:

$$\frac{\partial MR}{\partial t} = D_{eff}\left(\frac{\partial^2 MR}{\partial r^2}\right) \quad (3)$$

where, D_{eff} and t denote the effective diffusion coefficient, m^2/s and drying time, s. MR is the moisture content ratio, and r is diffusion path, m. The mathematical solution of Equation (5) in an infinite slab is given by:

$$MR = \frac{8}{\pi^2}\exp\left(\frac{-\pi^2 D_{eff} t}{4\delta^2}\right) \quad (4)$$

The effective moisture diffusivity was estimated from the slope of moisture ratio, using the following equation[13,30]:

$$\ln\frac{M_t}{M_0} = \ln\frac{8}{\pi^2} - \frac{\pi^2 D_{eff} t}{\delta^2} \quad (5)$$

D_{eff} can be calculated from the plot of ln (MR) versus t. Based on the best-fit linear curve, the slope and D_{eff} were computed from Equations (6) and (7):

$$slope = -\left(\pi^2 \frac{D_{eff}}{\delta^2}\right) \quad (6)$$

$$D_{eff} = -\frac{slope \times \delta^2}{\pi^2} \quad (7)$$

where, δ is the half-thickness of the sample, m.

2.4 Statistical analysis of the neural network model performance

The performance of the neural network model was assessed using the following four statistical metrics[30,31]:

$$MSE = \frac{1}{n}\sum_{i=1}^{n}(y_{cal,i} - y_{real,i})^2 \quad (8)$$

$$RMSE = \left[\frac{1}{n}\sum_{i=1}^{n}(y_{real,i} - y_{cal,i})\right]^{\frac{1}{2}} \quad (9)$$

$$MAPE = \frac{1}{n}\sum_{i=1}^{n}\frac{|y_{real,i} - y_{cal,i}|}{y_{real,i}} \times 100\% \quad (10)$$

$$R^2 = 1 - \frac{\sum_{i=1}^{n}(y_{real,i} - y_{cal,i})^2}{\sum_{i=1}^{n}(y_{reat,i} - y_{real,mean})^2} \quad (11)$$

where, n is the total number of experiments, and y_{real} and y_{cal} represent the measured and calculated moisture content (g water/g dry matter), respectively.

2.5 SSA improved BP neural network

This study developed a prediction network comprising four input neurons representing microwave power, relative humidity, drying time, and real-time mass, and two output neurons for moisture content and specific energy consumption (Figure 2). These four input variables have been demonstrated to significantly influence the microwave drying process[25,32,33], rendering them appropriate for predictive modeling. Addressing the limitations of traditional neural network design where the number of hidden layers and neurons is often determined by empirical formulas, which can restrict model accuracy, this research introduces a hybrid optimization approach. This method integrates a recurrent embedded error backpropagation algorithm with empirical guidelines to optimize the number of neurons within the hidden layers. The neural network architecture optimization was conducted through a systematic methodology combining theoretical principles and empirical analysis. Based on established engineering heuristics, the initial range for the number of hidden layer nodes was constrained between 3 and 12. A comprehensive optimization procedure was implemented to determine the optimal network topology by integrating the backpropagation (BP) algorithm with fundamental neural network design principles.

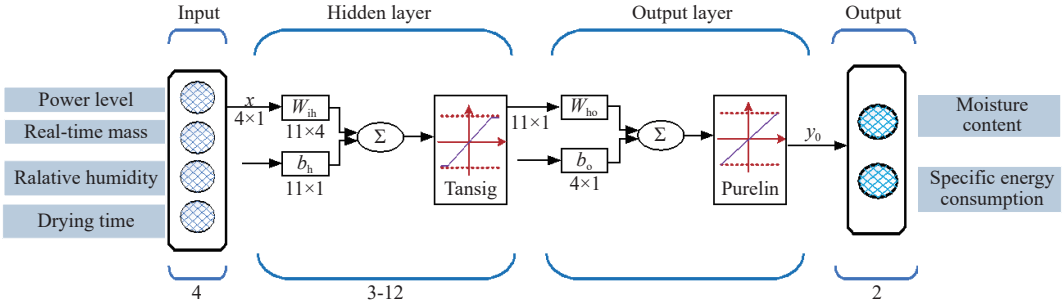

Figure 2 SSA-BP neural network prediction model

The performance of the network was evaluated using the mean squared error (MSE) as the primary metric. The results for various hidden layer configurations are presented in Table 1. Through iterative analysis, the optimal architecture was determined to consist of nine hidden layer neurons, achieving a minimum training error of 5.68×10^{-4}. The network architecture was further refined by employing the hyperbolic tangent sigmoid (tansig) activation function in both the input and hidden layers, while a linear transfer function (purelin) was utilized in the output layer to facilitate unrestricted output mapping.

2.6 Parameter optimization for SSA-BP

In this investigation, a serial structure was developed for the integrated prediction algorithm design. As illustrated in Figure 3, the algorithm architecture comprises three principal components: Hidden layer optimization, Sparrow Search Algorithm (SSA) optimization, and Back-Propagation (BP) neural network training. The execution of the algorithm can be divided into the following steps:

Table 1 Comparison of optimization for different hidden layer nodes

Hidden layer nodes	MSE	Hidden layer nodes	MSE
3	0.010 712	8	0.000 910
4	0.002 822	**9**	**0.000 568**
5	0.001 844	10	0.001 278
6	0.001 016	11	0.000 985
7	0.001 027	12	0.009 387

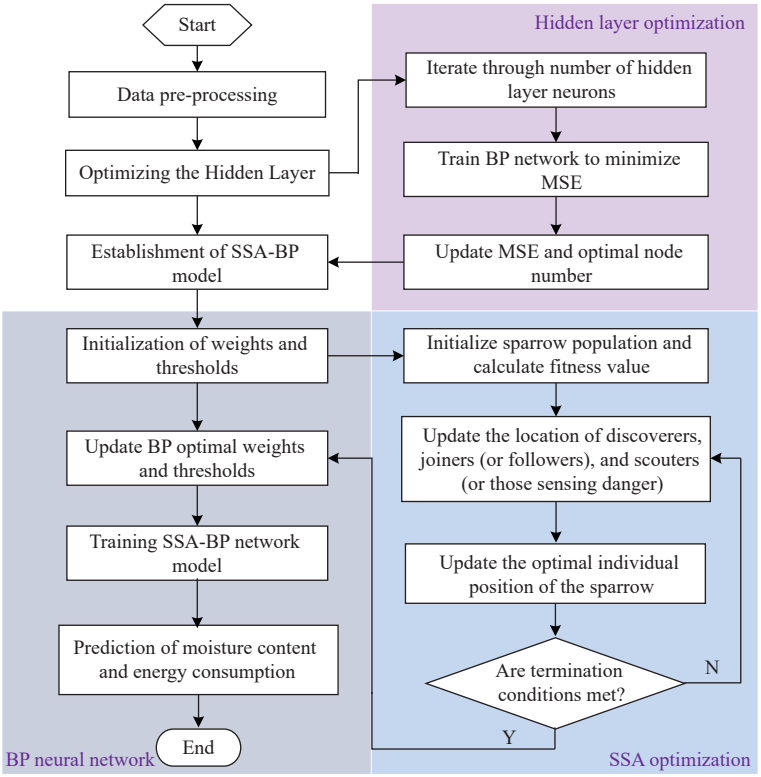

Figure 3 SSA-BP neural network flow

Step 1: Initialize the prediction network and utilize optimized iteration to determine the network structure.

Step 2: The algorithm calculates fitness values for each individual in the sparrow population, subsequently identifying the current optimal and worst fitness values along with their corresponding positional parameters. The position information of producer sparrows is updated according to Equation (12):

$$X_{i,j}^{t}=\begin{cases}X_{i,j}^{t}\cdot\exp\left(\dfrac{-i}{\alpha\cdot iter_{\max}}\right), & \text{if } R_2<\text{ST}\\ X_{i,j}^{t}+Q\cdot L, & \text{if } R_2\geq\text{ST}\end{cases}\tag{12}$$

where, t represents the current iteration number; $j=1,2,3,\ldots,d$ is the range of the optimization variable dimensions; $iter_{\max}$ denotes the maximum number of iterations; $X_{i,j}^{t}$ represents the position information of the i-th sparrow in the j-th dimension at the t-th iteration; R_2 is a random number within the range of 0 to 1; ST and α represent the safety threshold range and early warning value, respectively; Q is a random number drawn from a normal distribution; L is a $1\times j$ matrix with all elements equal to 1.

Step 3: The position information of joiner sparrows is updated according to Equation (13):

$$X_{i,j}^{t}=\begin{cases}Q\cdot\exp\left(\dfrac{X_{\text{worst}}-X_{i,j}^{t}}{i^2}\right), & \text{if } i>\dfrac{n}{2}\\ X_{i,j}^{t}+|X_{i,j}-X_{p}^{t+1}|\cdot A\cdot L, & \text{otherwise}\end{cases}\tag{13}$$

where, X_{p}^{t} represents the best foraging location of the producers; X_{worst} represents the worst foraging location of the producers. A are matrices satisfying specific optimization conditions $A^{+}=A^{T}(AA^{T})^{-1}$.

Step 4: The position information of scouters (early warning sparrows) is updated according to Equation (14):

$$X_{i,j}^{t+1}=\begin{cases}X_{\text{best}}^{t}+\beta\cdot|X_{i,j}^{t}-X_{\text{best}}^{t}|, & \text{if } f_i>f_g\\ X_{i,j}^{t}+K\cdot\dfrac{|X_{i,j}^{t}-X_{\text{worst}}^{t}|}{(f_i-f_w)+\varepsilon}, & \text{if } f_i=f_g\end{cases}\tag{14}$$

where, X_{best}^{t} represents the current global best position; β is a random number drawn from a standard normal distribution; $K\in(-1,1)$ is a random number that determines the direction of sparrow flight and relates to step length parameter adjustment; f_i is the current fitness value of the scouter; f_g and f_w are the current global best and worst fitness values, respectively; ε is a constant preventing zero-division errors.

Step 5: Select the individuals with better positions to update the

positions of the producers, gleaners, and early warnings, and calculate the fitness of the updated population.

Step 6: Calculate the population fitness and check if the termination condition is met. If yes, return the optimal thresholds and weights; otherwise, jump to Step 4 and continue the execution.

Step 7: Input the optimal thresholds and weights into the BP neural network structure, perform network training, and complete the prediction of moisture content and energy consumption.

3 Results and analysis

3.1 Influence of power level on effective moisture diffusivity

The experimental values of ln (MR) were plotted versus drying time (s) as shown in Figure 4. The experimental data were used to estimate the statistical best-fit and following relationships for each microwave power level.

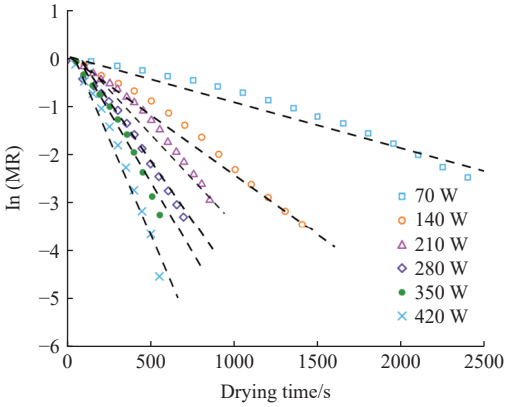

Figure 4 Variation of ln (MR) vs. drying time for beef muscle samples fried at different power levels

Based on the slope of curve for each power level, the effective diffusivity coefficient was calculated from Equations (6) and (7), and the results are presented in Table 2.

Table 2 Effective diffusivity of beef muscle at different power levels

Microwave power levels/W	Effective diffusivity/m²·s⁻¹
70	2.230×10^{-9}
140	4.994×10^{-9}
210	1.291×10^{-8}
280	1.771×10^{-8}
350	2.681×10^{-8}
420	2.870×10^{-8}

Microwave power level is a key factor influencing the effective moisture diffusion coefficient, as indicated in Table 2. The D_{eff} values reported here fall within the typical range of 10^{-12}-10^{-8} m²/s for food materials[34]. It was observed by Darvishi et al. that the D_{eff} values of microwave dried sardine fish were between 7.16×10^{-8} m²/s and 3.05×10^{-7} m²/s as the MW power level was increased from 200 to 500 W[22]. The increased heating from the higher microwave power density boosts the mobility and diffusion of the water molecules in the sample. As a result, this enhancement in moisture diffusivity allows the water to migrate more easily from the interior to the surface of the material. The regression equation of D_{eff} and microwave power was obtained as illustrated in Figure 5. From this illustration, it is evident that the relationship is linear and described by:

$$D_{eff} = 7.902\times10^{-9}P - 3.301\times10^{-9} \quad (R^2 = 0.9837) \qquad (15)$$

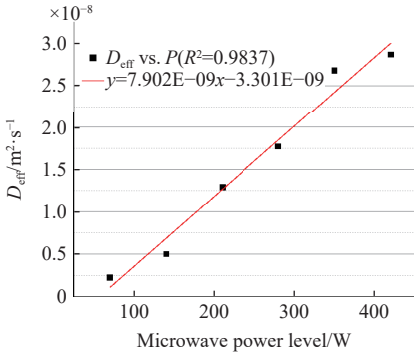

Figure 5 Influence of microwave power level on D_{eff} in beef muscle

3.2 Influence of drying parameters on microwave drying process of beef

3.2.1 Effect of power level on drying process modeling

The experimental data presented in Figure 6a describe the variation in moisture content of experimental samples during drying at six power levels (70 W, 140 W, 210 W, 280 W, 350 W, and 420 W). These results indicate that as the microwave power level increases, the slope of the drying curves rises, and the time required for samples to reach the same moisture content decreases[22]. During the early stages of drying, the microwave energy absorbing capacity was high due to the higher moisture content of the experimental samples. The larger quantities of energy increased the amount of water evaporated and the vapor pressure gradients within the sample. These vapor pressure gradients accelerate water vapor transport from the interior regions of the sample to the external surfaces[35].

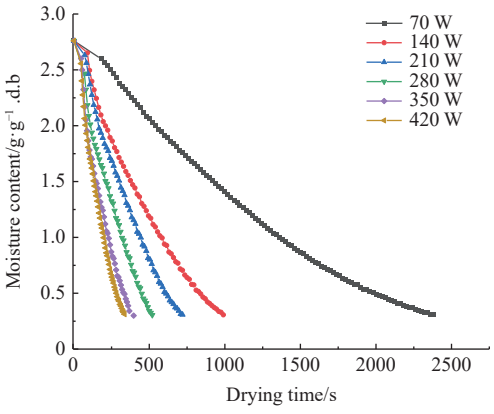

a. Drying curves at different power levels

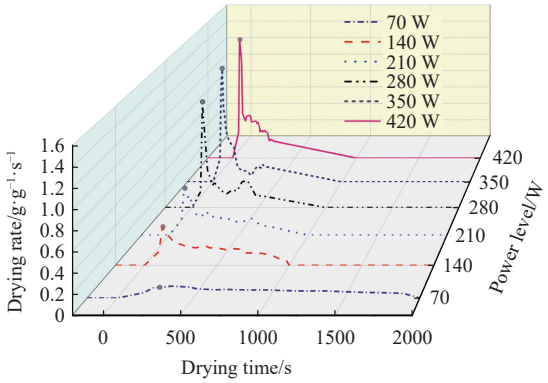

b. Drying rate curves at different power levels

Figure 6 Drying characteristics of beef muscle at different MW power levels

As the drying process continues, the decline in moisture content leads to a decrease in the vapor pressure gradients within the sample, resulting in a lower rate of drying as shown in Figure 6b. These observations are consistent with earlier literature, which indicates that during the microwave drying process, the migration of moisture within the sample is closely related to the internal liquid concentration gradient and the vapor pressure gradient[36]. The observations also confirm the significant impact of microwave power level on the rate of drying. Higher microwave power levels result in a faster drying process due to enhanced moisture evaporation and increased vapor pressure gradients within the sample[29,37].

3.2.2 Effect of relative humidity on microwave drying process of beef

Figure 7 illustrates the effect of relative humidity (0%, 30%, and 50%) on moisture content during microwave drying of lean beef samples at 350 W. The results demonstrate an inverse relationship between relative humidity and moisture removal rate. Higher relative humidity led to reduced vapor pressure gradients within the samples, resulting in decreased drying rates. While lower relative humidity levels achieved faster drying rates, higher vapor pressures near the sample surface during drying potentially improved the product structure[32]. The elevated relative humidity extended the drying time to reach target moisture content while preventing excessive surface dehydration.

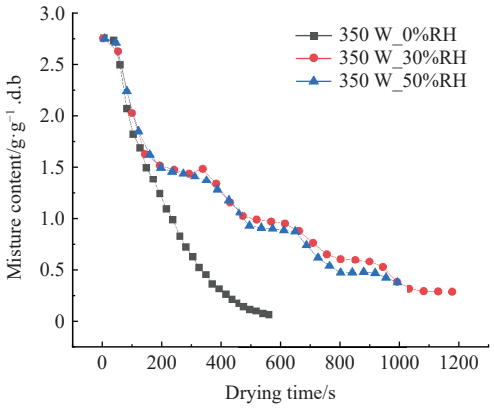

a. Drying curves at different relative humidities

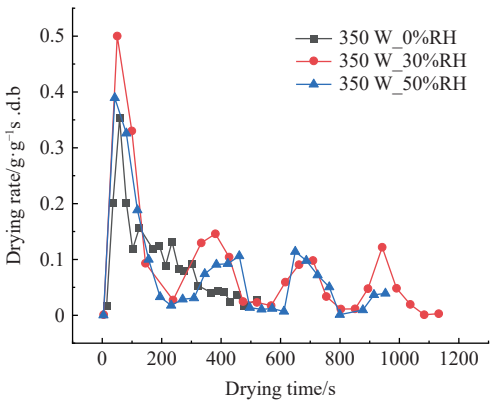

b. Drying rate curves at different relative humidities

Figure 7 Drying characteristics of beef muscle at different relative humidities

3.2.3 Effect of power level on energy consumption

Prior investigations have consistently emphasized the significant influence of microwave power level on specific energy consumption (SEC) during drying processes[29]. Since optimizing energy consumption while maximizing moisture removal efficiency is crucial for drying process modeling, a thorough evaluation of energy utilization in microwave-assisted beef muscle drying was conducted. The relationship between SEC and moisture content is illustrated in Figure 8. The final SEC values ranged from 8.9 to 11.9 MJ/kg of water, with similar trend patterns observed across different microwave power levels. The SEC curves exhibited stabilization as the sample moisture content decreased, particularly after the initial ramp-up drying phase. This phenomenon can be attributed to reduced microwave energy absorption as the moisture content diminishes during the later stages of drying[38]. Consequently, more energy is required to remove an equivalent mass of water in the final drying stages compared to the initial phases, a finding consistent with previous studies on microwave drying of Ficus carica Linn leaves[12]. The results indicate that at equivalent moisture contents, higher microwave power levels correspond to lower energy consumption during the drying process. However, excessive microwave power can result in sample charring, corroborating previous findings from research on sardine and mussel drying[22,29].

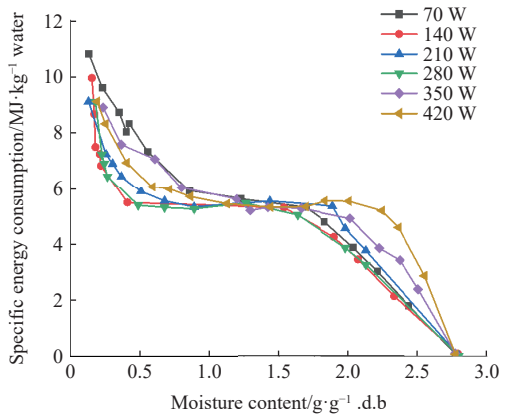

Figure 8 Effect of microwave power and drying time on specific energy consumption

As shown in the overall energy consumption change trend line in Figure 9, the final average unit energy consumption reaches a maximum of 10.46 MJ/kg water at a microwave power of 70 W, and a minimum of 8.39 MJ/kg water at a microwave power of 420 W.

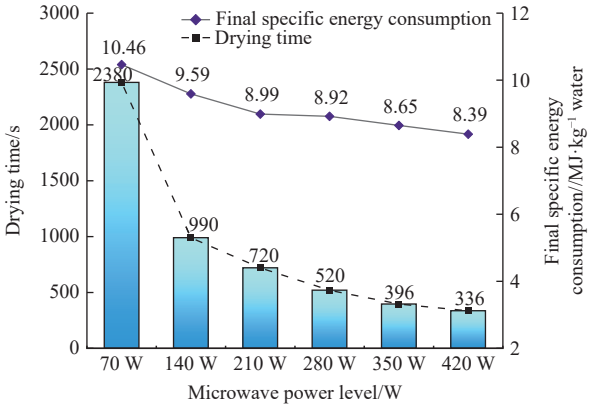

Figure 9 Variation of drying time and energy consumption under different microwave power levels

3.3 SSA-BP neural network model validation

The SSA-BP neural network prediction algorithm was created in MATLAB, with 409 groups of training sets. To assess the network's performance, the predicted values were visualized

through plotting. Figure 10 illustrates the results for the most effective network in modeling and predicting the variations in moisture content and specific energy consumption of the samples during the drying process. The findings indicate that the SSA-BP model accurately predicts both moisture content and specific energy consumption during the microwave drying process.

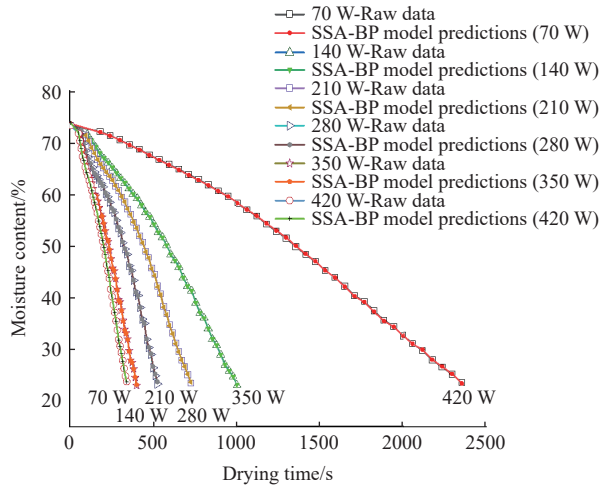

a. Prediction result of moisture content

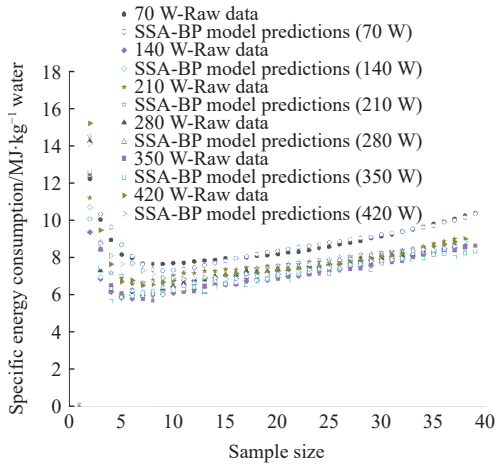

b. Prediction result of specific energy consumption

Figure 10 Comparison of optimized SSA-BP model predictions and measured results at different power levels

Experimental data on the moisture content of beef muscle samples over time at a microwave power of 280 W were randomly selected for model validation. The outcomes in Figure 11 provide the MSE (mean square error) change of the SSA-BP model during system training, validation, and testing. The smaller magnitudes of MSE represent more accurate predictions by the model. As is evident, the overall MSE decreases consistently and eventually ends after the 155th iteration, and with the MSE reaching a minimum value of 2.211E-4. The regression plots related to the training, validation, testing, and overall performance of the network are presented in Figure 12. The fit across all datasets was quite robust, with correlation coefficients approaching 1. An analysis of the data point distribution reveals that nearly all points are closely aligned along the 45° line, indicating a strong agreement between the network outputs and the targets. Notably, the correlation coefficient for the training data is 0.999 11, while the coefficients for validation, testing, and the overall neural network process were 0.998 81, 0.998 37, and 0.998 92, respectively. These performance metrics suggest that the designed SSA-BP neural network is capable of effectively predicting moisture content and specific energy consumption during the drying process of beef slices.

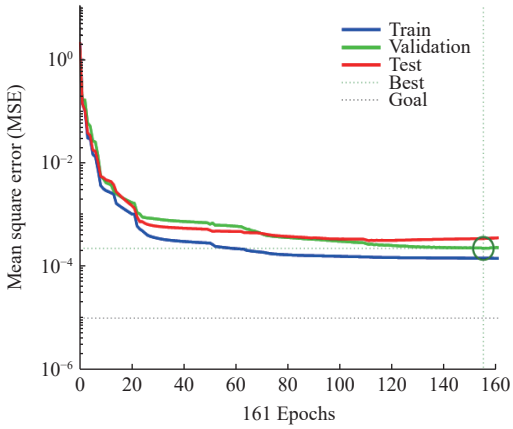

Figure 11 System mean square error curve of SSA-BP model (280 W)

To confirm the accuracy and stability of the SSA-BP model prediction for changes in moisture content of beef during microwave drying, a comparison with outcomes from the BP[39], GA-BP[40], and the SSA-BP model was conducted. The present study theoretically evaluated the model relevance and prediction accuracy, employing R-squared (R^2) and root mean square error (RMSE) as metrics for model relevance verification, and mean absolute percentage error (MAPE) as a metric for model prediction accuracy verification. The goodness of fit, RMSE, and MAPE of the BP model, GA-BP model, and the SSA-BP prediction model are comparatively presented in Table 3. The results indicate that the SSA-BP model effectively predicts the moisture content of beef muscle slices during microwave drying. The RMSE, MAPE, and R^2 values for the SSA-BP model were found to be 0.2354, 3.7604, and 0.9821, respectively.

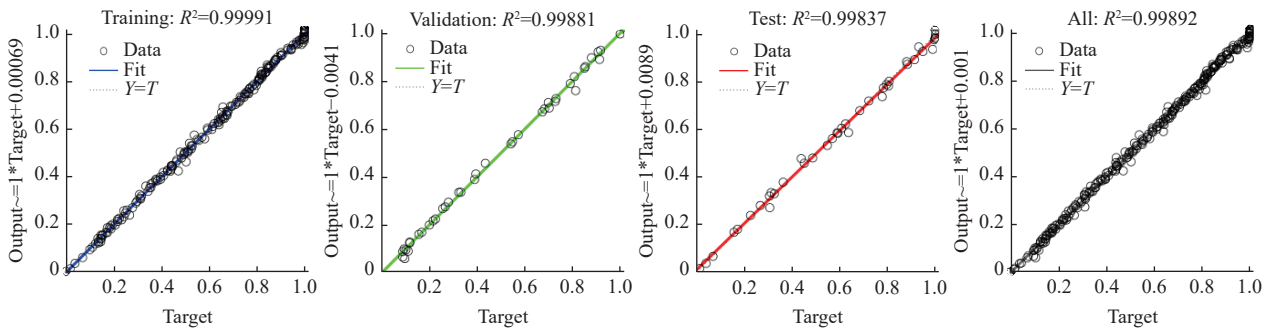

Figure 12 SSA-BP neural network model with training, validation, test, and all prediction set

Table 3 Comparative analysis of model predictive performance

Model	Moisture content			Specific energy consumption		
	R^2	RMSE	MAPE/%	R^2	RMSE	MAPE/%
BP	0.9972	0.7849	1.4172	0.9352	0.450 90	6.1722
GA-BP	0.9988	0.5268	0.9701	0.9434	0.433 47	4.9425
SSA-BP	0.9999	0.1247	0.2091	0.9821	0.235 40	3.7604

4 Conclusions

This study demonstrated an effective approach for modeling and optimizing microwave drying of beef muscle. The experimental investigation revealed moisture diffusivity values ranging from 2.23×10^{-9} to 2.87×10^{-9} m²/s, with minimal specific energy consumption (8.39 MJ/kg water) achieved at 420 W microwave power. These findings provide valuable insights into both drying kinetics and energy efficiency parameters critical for industrial applications.

A novel SSA-optimized BP neural network model was developed to accurately predict moisture content during variable microwave power drying. The multi-objective Sparrow Search Algorithm effectively optimized the initial weights and thresholds of the neural network, resulting in superior predictive performance compared to conventional approaches. Validation metrics confirmed the model's exceptional accuracy (RMSE: 0.2354, MAPE: 3.7604%, R^2: 0.9821), demonstrating significant improvements over traditional BP neural networks and GA-optimized BP networks.

The proposed modeling framework establishes a robust foundation for process optimization in microwave-based food dehydration systems. The integration of SSA optimization with neural network modeling presents a promising approach for intelligent control systems in industrial-scale microwave drying operations, potentially leading to improved product quality and energy efficiency in commercial food processing applications.

Acknowledgements

This work was supported by the 2024 Tertiary Education Scientific Research Project of the Guangzhou Municipal Education Bureau (Grant No. 2024312026), a grant from the Sugar Creek Packing Company, and the Dale A. Seiberling Endowment to the Food Engineering Research Laboratory at The Ohio State University.

Data Availability Statement

The data that support the findings of this study are available from the corresponding author upon reasonable request.

[References]

[1] Zia Q, Alawami M, Mokhtar N F K, Nhari R M H R, Hanish I. Current analytical methods for porcine identification in meat and meat products. Food Chemistry, 2020; 324: 126664.

[2] Kim S-M, Kim T-K, Cha JY, Kang M-C, Lee J H, Yong H I, et al. Novel processing technologies for improving quality and storage stability of jerky: A review. Lwt, 2021; 151: 112179.

[3] Muga F C, Marenya M O, Workneh T S. Modelling the thin-layer drying kinetics of marinated beef during infrared-assisted hot air processing of biltong. International Journal of Food Science, 2021; doi: 10.1155/2021/8819780.

[4] Choi Y-S, Jeong J-Y, Choi J-H, Han D-J, Kim H-Y, Lee M-A, et al. Effect of packaging methods on the quality properties of stick type restructured jerky. Korean Journal for Food Science of Animal Resources, 2007; 27(3): 290–298.

[5] Elmas F, Bodruk A, Köprüalan Ö, Arıkaya Ş, Koca N, Serdaroğlu F M, et al. Drying kinetics behavior of turkey breast meat in different drying methods. Journal of Food Process Engineering, 2020; 43(10): e13487

[6] Dev S R S, Geetha P, Orsat V, Gariépy Y, Raghavan G S V. Effects of microwave-assisted hot air drying and conventional hot air drying on the drying kinetics, color, rehydration, and volatiles of Moringa oleifera. Drying Technology, 2011; 29(12): 1452–1458.

[7] Rajkumar G, Shanmugam S, de Sousa Galvão M, Leite Neta M T S, Dutra Sandes R D, Mujumdar A S, et al. Comparative evaluation of physical properties and aroma profile of carrot slices subjected to hot air and freeze drying. Drying Technology, 2017; 35(6): 699–708.

[8] Süfer Ö, Palazoğlu T K. A study on hot-air drying of pomegranate: Kinetics of dehydration, rehydration and effects on bioactive compounds. Journal of Thermal Analysis and Calorimetry, 2019; 137: 1981–1990.

[9] Abano E E. Kinetics and quality of microwave‐assisted drying of mango (Mangifera indica). International Journal of Food Science, 2016; 2016(1): 2037029.

[10] Dzelagha B F, Ngwa N M, Nde Bup D. A review of cocoa drying technologies and the effect on bean quality parameters. International Journal of Food Science, 2020; 2020(1): 8830127.

[11] Wray D, Ramaswamy H S. Novel concepts in microwave drying of foods. Drying Technology, 2015; 33(7): 769–783. doi: 10.1080/ 07373937. 2014.985793

[12] Yilmaz P, Demirhan E, Özbek B. Microwave drying effect on drying characteristic and energy consumption of Ficus carica Linn leaves. Journal of Food Process Engineering, 2021; 44(10): e13831.

[13] Çelen S. Effect of microwave drying on the drying characteristics, color, microstructure, and thermal properties of Trabzon persimmon. Foods, 2019; 8(2): 84.

[14] Filipović I, Ćurčić B, Filipović V, Nićetin M, Filipović J, Knežević V. The effects of technological parameters on chicken meat osmotic dehydration process efficiency. Journal of Food Processing and Preservation, 2017; 41(1): e13116.

[15] Bai J W, Xiao H W, Ma H L, Zhou C-S. Artificial neural network modeling of drying kinetics and color changes of Ginkgo Biloba seeds during microwave drying process. Journal of Food Quality, 2018; 2018(1): 3278595.

[16] Onu C E, Igbokwe P K, Nwabanne J T, Nwajinka C O, Ohale P E. Evaluation of optimization techniques in predicting optimum moisture content reduction in drying potato slices. Artificial Intelligence in Agriculture, 2020; 4: 39–47.

[17] Sarimeseli A, Coskun M A, Yuceer M. Modeling microwave drying kinetics of thyme (T hymus Vulgaris L.) leaves using ann methodology and dried product quality. Journal of Food Processing and Preservation, 2014; 38(1): 558–564.

[18] Marić L, Malešić E, Tušek A J, Benković M, Valinger D, Jurina T, et al. Effects of drying on physical and chemical properties of root vegetables: Artificial neural network modelling. Food and bioproducts processing. 2020; 119: 148–160. doi:10.1016/j.fbp.2019.11.002

[19] Raj G V S B, Dash K K. Microwave vacuum drying of dragon fruit slice: Artificial neural network modelling, genetic algorithm optimization, and kinetics study. Computers and Electronics in Agriculture, 2020; 178: 105814.

[20] Karami H, Kaveh M, Mirzaee‐Ghaleh E, Taghinezhad E. Using PSO and GWO techniques for prediction some drying properties of tarragon (*Artemisia dracunculus* L.). Journal of Food Process Engineering, 2018; 41(8): e12921.

[21] Wang T X, Ying X Y, Zhang Q, Xu Y R, Jiang C H, Shang J W, et al. Drying kinetics prediction and quality effect of ultrasonic synergy vacuum far‐infrared drying of Codonopsis pilosula. Journal of Food Science, 2024; 89: 966–981.

[22] Darvishi H, Azadbakht M, Rezaeiasl A, Farhang A. Drying characteristics of sardine fish dried with microwave heating. Journal of the Saudi Society of Agricultural Sciences, 2013; 12: 121–127.

[23] AOAC. Official methods of analysis of AOAC International (16th edn). In: Patricia A. Elsevier. 1995.192p

[24] Heinz G, Hautzinger P. Meat processing technology for small-to medium-scale producers. Rap Publication. 2007.87p

[25] Pu H J, Li Z F, Hui J, Vijaya Raghavan G S. Effect of relative humidity on microwave drying of carrot. Journal of Food Engineering, 2016; 190: 167–175.

[26] Ju H-Y, El-Mashad H M, Fang X-M, Pan Z, Xiao H-W, et al. Drying characteristics and modeling of yam slices under different relative humidity

conditions. Drying Technology, 2016; 34: 296–306.
[27] Li J, Li Z F, Raghavan G S V, Song F H, Song C F, Liu M B, et al. Fuzzy logic control of relative humidity in microwave drying of hawthorn. Journal of Food Engineering, 2021; 310: 110706.
[28] Soysal Y, Öztekin S, Eren Ö. Microwave drying of parsley: modelling, kinetics, and energy aspects. Biosystems Engineering, 2006; 93(4): 403–413.
[29] Kipcak A S. Microwave drying kinetics of mussels (Mytilus edulis). Research on Chemical Intermediates, 2017; 43(3): 1429–1445.
[30] Beigi M, Torki M. Experimental and ANN modeling study on microwave dried onion slices. Heat and Mass Transfer, 2020; 57: 787–796.
[31] Taki M, Farhadi R. Modeling the energy gain reduction due to shadow in flat-plate solar collectors; Application of artificial intelligence. Artificial Intelligence in Agriculture, 2021; 5: 185–195.
[32] Xu W X, Islam M N, Cao X H, Tian J H, Zhu G Y. Effect of relative humidity on drying characteristics of microwave assisted hot air drying and qualities of dried finger citron slices. LWT, 2021; 137: 110413.
[33] Silva E G, Gomez R S, Gomes J P, Silva W P, Porto K Y, Rolim F D, et al. Heat and mass transfer on the microwave drying of rough rice grains: An experimental analysis. Agriculture, 2020; 11(1): 1–17.
[34] Doymaz İ. Evaluation of some thin-layer drying models of persimmon slices (*Diospyros kaki* L.). Energy Conversion and Management, 2012; 56: 199–205.
[35] Rout R K, Kumar A, Rao P S. A comparative assessment of drying kinetics, energy consumption, mathematical modeling, and multivariate analysis of Indian borage (*Plectranthus amboinicus*) leaves. Journal of Food Process Engineering, 2024; 47(5): e14630.
[36] Feng H, Yin Y, Tang J M. Microwave drying of food and agricultural materials: basics and heat and mass transfer modeling. Food Engineering Reviews, 2012; 4: 89–106.
[37] Kipcak A S, Ismail O. Microwave drying of fish, chicken and beef samples. J Food Sci Technol, 2021; 58: 281–291.
[38] Choo C O, Chua B L, Figiel A, Jałoszyński K, Wojdyło A, Szumny A, et al. Hybrid drying of Murraya koenigii leaves: Energy consumption, antioxidant capacity, profiling of volatile compounds and quality studies. Processes, 2020; 8(2): 240.
[39] Sun Q, Zhang M, Yang P Q. Combination of LF-NMR and BP-ANN to monitor water states of typical fruits and vegetables during microwave vacuum drying. Lwt, 2019; 116: 108548.
[40] Zhang K Q, Wang X L, Wang N F. Moisture prediction of municipal sludge drying process using BP neural network modeling and genetic algorithm optimization. Research Square, 2024; In press. doi: 10.21203/rs.3.rs-3708102/v1.